


# ***PhysHand: A Hand Simulation Model with Physiological Geometry, Physical Deformation, and Accurate Contact Handling***

Mingyang Sun<sup>†,1</sup>, Dongliang Kou<sup>†,1</sup>, Ruisheng Yuan<sup>1</sup>, Dingkan Yang<sup>1</sup>, Peng Zhai<sup>1</sup>, Xiao Zhao<sup>1</sup>,  
Yang Jiang<sup>1</sup>, Xiong Li<sup>4</sup>, Jingchen Li<sup>‡,4</sup>, and Lihua Zhang<sup>‡,1,2,3</sup>

<sup>1</sup>Academy for Engineering and Technology, Fudan University, Shanghai, China.

<sup>2</sup>Engineering Research Center of AI and Robotics, Ministry of Education, Changchun, China.

<sup>3</sup>Jilin Provincial Key Laboratory of Intelligence Science and Engineering, Changchun, China.

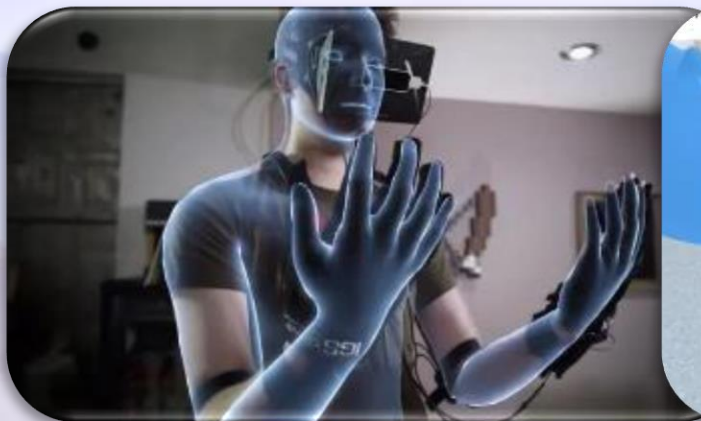
<sup>4</sup>Tencent Robotics X Lab, Shenzhen, China.

**Speaker:** Mingyang Sun (孙铭阳)

**Colleague:** Dongliang Kou (寇栋梁)

**Department:** Fudan University (复旦大学), Shanghai, China

In virtual Hand-Object Interaction (HOI), the authenticity of the hand's **deformation** is important:



[1]

Immersive  
experience



[2]

Accurate  
manipulation



[3]

Tactile  
feedback

[1] <https://baijiahao.baidu.com/s?id=1763406672043028291&wfr=spider&for=pc>

[2] <https://xsj.699pic.com/sou/nagongjudeshou.html>

[3] [https://www.sohu.com/a/392493099\\_427506](https://www.sohu.com/a/392493099_427506)



## Challenges



### Hand Simulator

**Geometry**

**Physics**

**Contact**

The human hand possesses a layered structure comprising bones, muscles, fat, and skin.



## Challenges



### Hand Simulator

**Geometry**

**Physics**

**Contact**

The skeleton is rigid, but the skin and flesh exhibit distinct non-rigid behaviors.





## Challenges



## Hand Simulator

**Geometry**

**Physics**

**Contact**

Rich contacts always imply overlap in HOI, posing challenges for accurate and fast collision detection and correction.



## 2. Related works



Research	Hand Layer			Deformation	Contact Handling
	Skin	Flesh	Skeleton		
Ott <i>et al.</i> [OVT10]	✓	-	-	Skinning weights	Mesh
Jacobs <i>et al.</i> [JSF12]	✓	-	-	Skinning weights	Mesh
Wang <i>et al.</i> [WML24]	✓	-	-	Skinning weights	SDF
Jacobs <i>et al.</i> [JF11]	✓	✓	-	Linear elasticity	Mesh
Hirota <i>et al.</i> [HT16]	✓	✓	-	Linear elasticity	Mesh
Garre <i>et al.</i> [GHGO11]	✓	✓	Box	Linear elasticity	Mesh
Verschoor <i>et al.</i> [VLO18]	✓	✓	Capsule	Linear elasticity	SDF
Sorli <i>et al.</i> [SCV*21]	✓	✓	Capsule	Linear elasticity	SDF
Akihiko <i>et al.</i> [MYHYH17]	✓	✓	Mesh	Linear elasticity	-
PhysHand (ours)	✓	✓	Detailed mesh	Layer-corresponding constraints	SDF with multi-resolution querying

Unrealistic deformation arises from simplified hand **geometry**, neglect of the different **physics** attributes of the hand, and penetration due to imprecise **contact** handling.

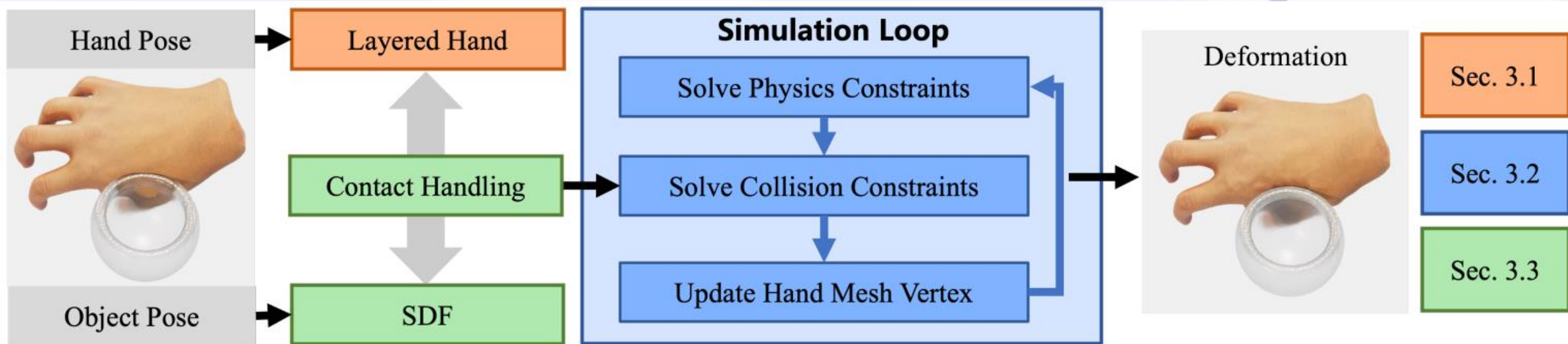


**Figure 2:** Schematic overview of the PhysHand. The pose of hand and object can be obtained by manual setup or from a generative model [LZY\*23]. The layered hand serves as a simulation entity, governed by the simulation loop. The simulation loop updates the vertices of the hand model by solving constraints, where the collision constraints are generated by the contact handling module when the hand comes into contact with the object.

To address these problems, we propose **PhysHand**, a novel hand simulation model, which enhances the realism of deformation in HOI.



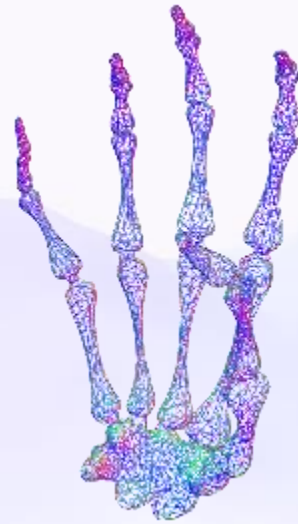
### 3. Method

#### Geometry

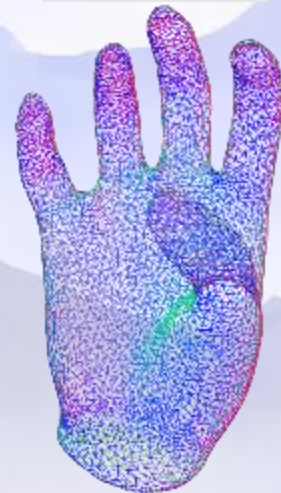
Generate hands with  
layered structure.

**NIMBLE[1]**

$$\mathcal{G}(\theta, \beta) = LBS(\mathcal{W}, J_p, \theta, \bar{T}).$$

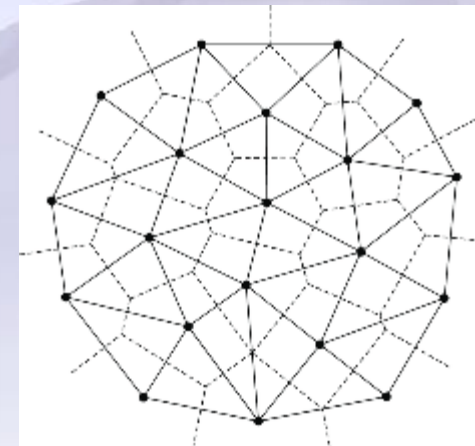


Skeleton



Skin

**Delaunay  
triangulation**



Textured geometry



Flesh

[1] Nimble: a non-rigid hand model with bones and muscles. ACM Transactions on Graphics (TOG), 41(4), 1-16.



## Physics

### ● Linear blend skinning for the skeleton

For the **skeleton** layer, we adopt skinning weights of the skeletal vertices derived from NIMBLE to calculate rigid body motions.

### ● XPBD for the flesh and skin

For the **flesh** and the **skin**, we adopt XPBD[1] as our dynamics framework with carefully designed **layer-corresponding constraints** to maintain flesh attached and skin smooth.

[1] XPBD: position-based simulation of compliant constrained dynamics. In Proceedings of the 9th International Conference on Motion in Games (pp. 49-54).

#### Algorithm 1 XPBD simulation for a single time step.

```
1:  $h \leftarrow \Delta t / \text{numSubSteps}$  ▷ Substep size
2: for  $i = 1, \dots, \text{numSubSteps}$  do ▷ Iteration
3:   initialize solution  $\mathbf{x} \leftarrow \mathbf{x}^i + h\mathbf{v}^i + h^2\mathbf{M}^{-1}\mathbf{f}_{\text{ext}}(\mathbf{x}^i)$ 
4:   initialize multipliers  $\lambda \leftarrow 0$ 
5:    $\tilde{\alpha} \leftarrow \frac{1}{h^2}\alpha$ 
6:   collision detection and correction ▷ Sec. 3.3
7:   for all constraints do
8:      $\mathbf{A} \leftarrow \nabla C(\mathbf{x})\mathbf{M}^{-1}\nabla C^T(\mathbf{x}) + \tilde{\alpha}$ 
9:      $\Delta\lambda \leftarrow -\mathbf{A}^{-1}(C(\mathbf{x}) + \tilde{\alpha}\lambda)$ 
10:     $\Delta\mathbf{x} \leftarrow \mathbf{M}^{-1}\nabla C^T(\mathbf{x})\Delta\lambda$  ▷ Projection
11:     $\lambda \leftarrow \lambda + \Delta\lambda$ 
12:     $\mathbf{x} \leftarrow \mathbf{x} + \Delta\mathbf{x}$ 
13:   end for
14:   update positions  $\mathbf{x}^{i+1} \leftarrow \mathbf{x}$ 
15:   update velocities  $\mathbf{v}^{i+1} \leftarrow \frac{\mathbf{x}^{i+1} - \mathbf{x}^i}{h}$ 
16:    $i \leftarrow i + 1$ 
17: end for
```



## Physics

### ➤ Layer-corresponding constraints

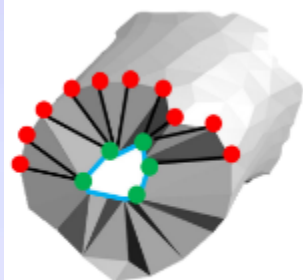
#### Basic Constraints

$$C^{\text{edge}}(\mathbf{x}_1, \mathbf{x}_2) = \|\mathbf{x}_1 - \mathbf{x}_2\| - L,$$

→ Edge length preserving

$$C^{\text{tet}}(\mathbf{x}_1, \mathbf{x}_2, \mathbf{x}_3, \mathbf{x}_4) = \mathbf{x}_2 - \mathbf{x}_1 \times \mathbf{x}_3 - \mathbf{x}_4 - 6V.$$

→ Tetrahedron volume preserving



- Flesh vertices
- Skeleton vertices
- Shared edges

(a)  $C^{\text{att}}$

$$C^{\text{att}}(\mathbf{x}_{\text{flesh}}) = C^{\text{edge}}(\mathbf{x}_{\text{flesh}}, \mathbf{x}_{\text{skeleton}}),$$

$$\mathbf{x}_{\text{skeleton}} = \arg \min_{\mathbf{x}_i \in S_{\text{skeleton}}} \|\mathbf{x}_{\text{flesh}, i}\|,$$

where  $S_{\text{skeleton}}$  is the set of vertices belong to the skeleton.

### (a) Flesh Attachment Constraint

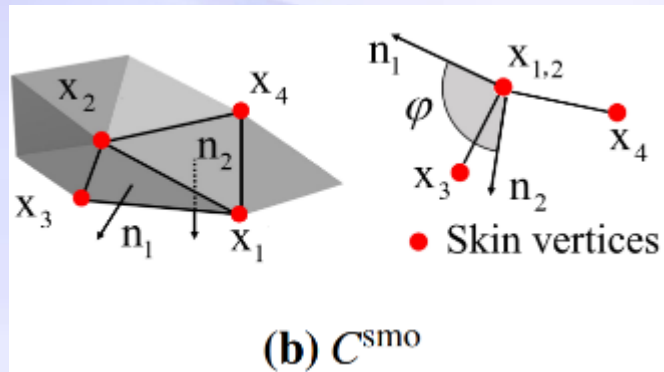
Each vertex of the flesh layer establishes an edge constraint with the nearest skeleton vertex to prevent excessive deformation.

## Physics

### ➤ Layer-corresponding constraints

Basic Constraints

$$\left\{ \begin{array}{l} C^{\text{edge}}(\mathbf{x}_1, \mathbf{x}_2) = \|\mathbf{x}_{1,2}\| - L, \longrightarrow \text{Edge length preserving} \\ C^{\text{tet}}(\mathbf{x}_1, \mathbf{x}_2, \mathbf{x}_3, \mathbf{x}_4) = \mathbf{x}_{2,1} \times \mathbf{x}_{3,1} \cdot \mathbf{x}_{4,1} - 6V. \longrightarrow \text{Tetrahedron volume preserving} \end{array} \right.$$



$$C^{\text{smo}}(\mathbf{x}_1, \mathbf{x}_2, \mathbf{x}_3, \mathbf{x}_4) = \arccos(\mathbf{n}_1 \cdot \mathbf{n}_2) - \varphi,$$

where  $\mathbf{x}_1, \mathbf{x}_2, \mathbf{x}_3$ , and  $\mathbf{x}_4$  are vertices that belong to two triangles with a shared edge,  $\mathbf{n}_1$  and  $\mathbf{n}_2$  are triangle normals and  $\varphi$  is the initial dihedral angle. We apply  $C^{\text{smo}}$  to the skin.

### (b) Skin Smoothness Constraint

For the skin layer, we keep the dihedral angle of adjacent triangles through normal vectors to provide smoothness.



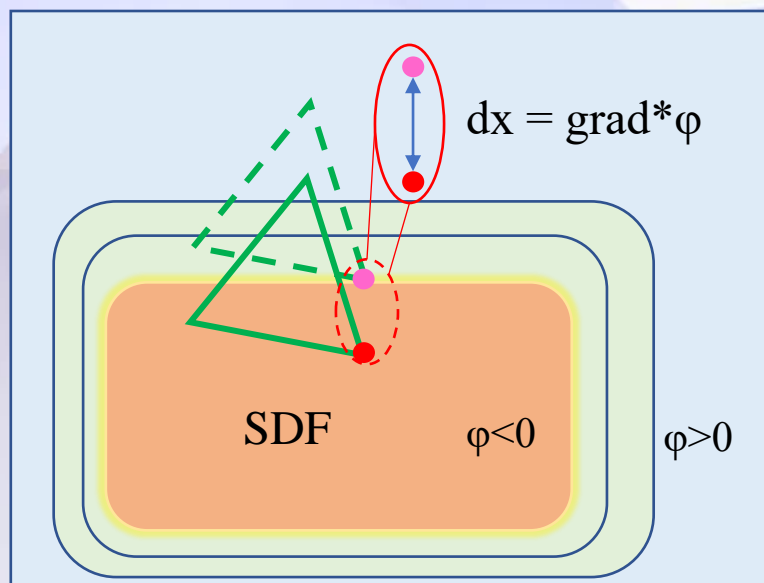
## Contact

### ➤ Analysis for SDF-based collision detection

#### ● SDF Representation

- The zero-level-set of an SDF can implicitly describe the surface of an object:

$$\mathcal{S} = \{\phi(\mathbf{x})\} = 0,$$



#### ● SDF for collision detection

- The collision constraint can be defined directly by the SDF.

$$C^{\text{coll}}(\mathbf{x}) = \phi(\mathbf{x}).$$

Collision constraint

When  $C^{\text{coll}}(\mathbf{x}) \leq 0$ , penetration occurs, then  $\mathbf{x}$  needs to be projected to  $\mathbf{x}'$  that satisfies the collision constraint:

$$\mathbf{x}' = \mathbf{x} - \frac{\nabla\phi(\mathbf{x})}{\|\nabla\phi(\mathbf{x})\|} \phi(\mathbf{x}),$$

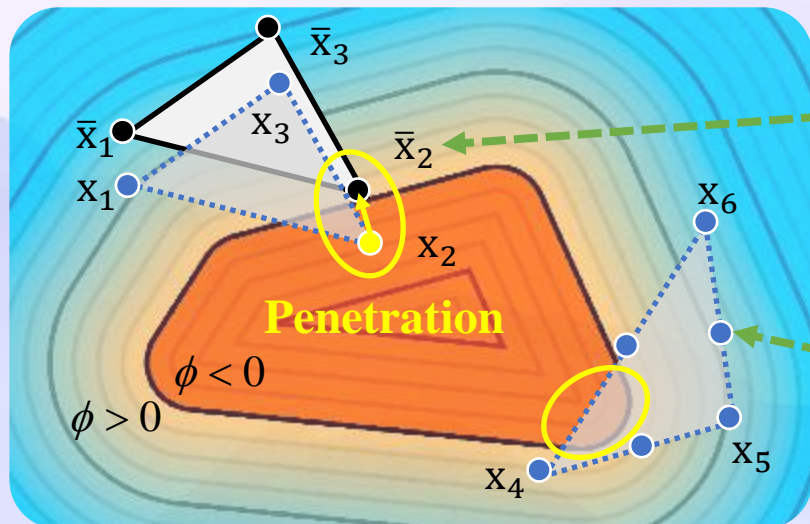
Correction projection





## Contact

### ➤ Analysis for SDF-based collision detection



- Given a triangle, the **TARGET** is to find a point on the triangle to represent its minimum signed distance value, so that the **penetrated** triangle can be projected to the **penetration-free** position.

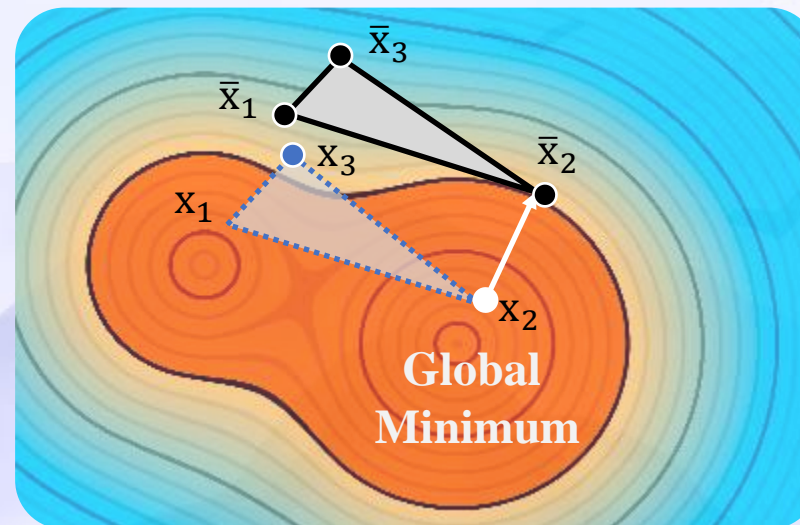
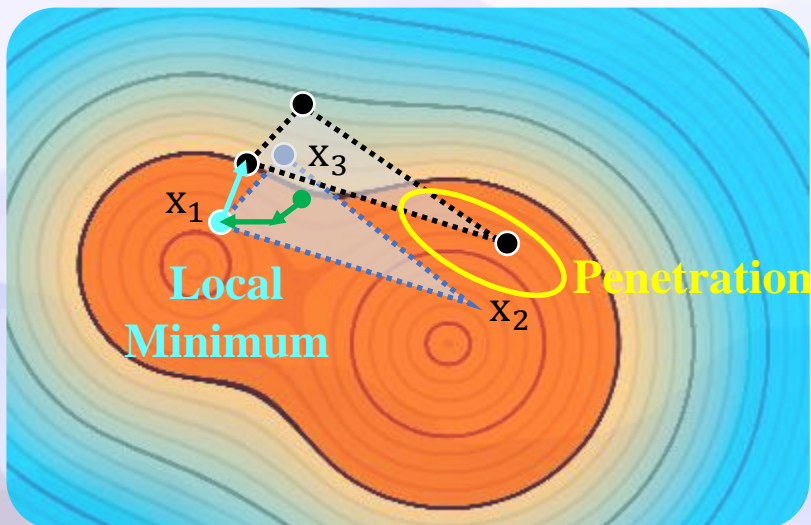
#### (a) **Vanilla method: vertex-SDF [1]**

For a triangle, the signed distances of its vertices and centers of edges fail to precisely depict its penetration state.



## Contact

### ➤ Analysis for SDF-based collision detection



### (b) Optimization-based method: opt-SDF [1]

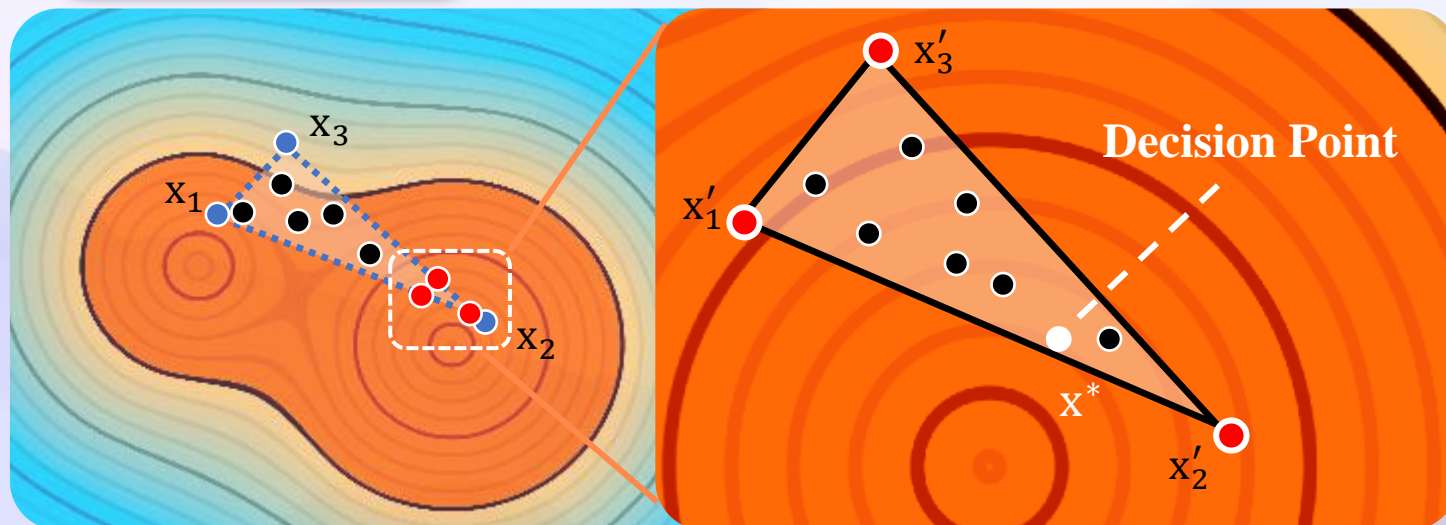
- It iteratively solves for an **optimal point (green points and arrows)** with the lowest signed distance.
- However, SDF is usually nonlinear, which makes opt-SDF sensitive to initial guesses and susceptible to converging towards **local optima (bright blue point)**, leading to an insufficient correction.
- Instead, the **global optimum (white point)** can help eliminate penetration.

[1] Macklin, M., Erleben, K., Müller, M., Chentanez, N., Jeschke, S., & Corse, Z. (2020). Local optimization for robust signed distance field collision. Proceedings of the ACM on Computer Graphics and Interactive Techniques, 3(1), 1-17.



## Contact

### ➤ Analysis for SDF-based collision detection



**Algorithm 2** Contact handling with multi-resolution querying.

```

1: for all triangles of the skin do
2:    $T = \{x_1, x_2, x_3\}$ 
3:   for  $i = 1, \dots$ , sampling times do
4:     query the sampled points  $\mathcal{X}$  on triangle  $T$ 
5:     obtain the triangle  $T' = \{x'_1, x'_2, x'_3\}$  with the lowest
       three signed distances.
6:      $T \leftarrow T'$ 
7:   end for
8:   obtain the decision point  $x^* \leftarrow \underset{x}{\operatorname{argmin}} \phi(\mathcal{X})$ 

```

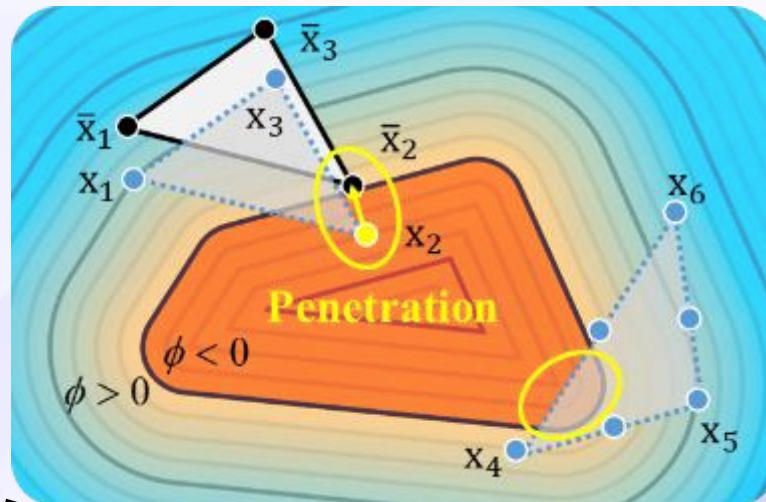
### (c) Multi-resolution method (ours): multi-res-SDF

- We perform global **sampling** on the triangle (*left*), then select **three points (red points)** with the lowest signed distance to form a new triangle (*right*), iteratively increasing the resolution.
- After the final sampling iteration, we select the point with the smallest signed distance as the decision point  $x^*$ , which is more likely to approach the global optimum.
- Typically 2 sampling iteration is enough.

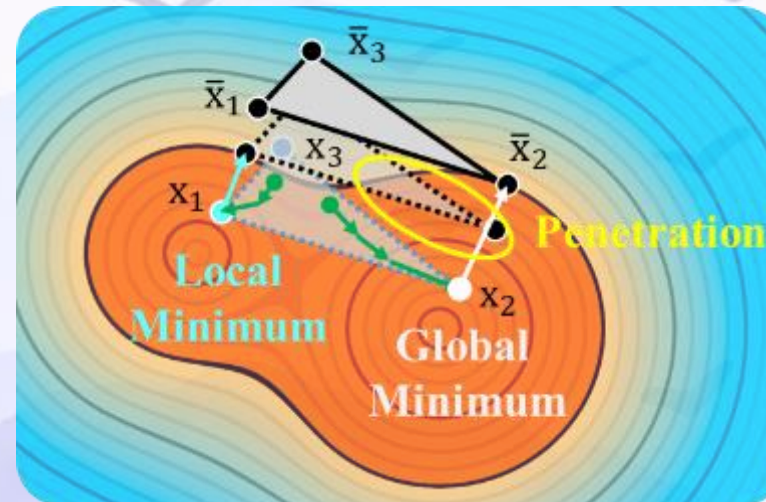


## Contact

Low resolution



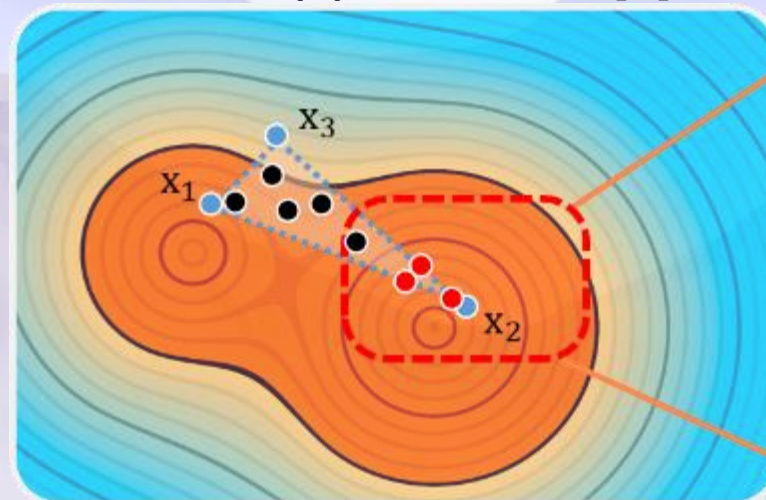
(a) vertex-SDF [1]



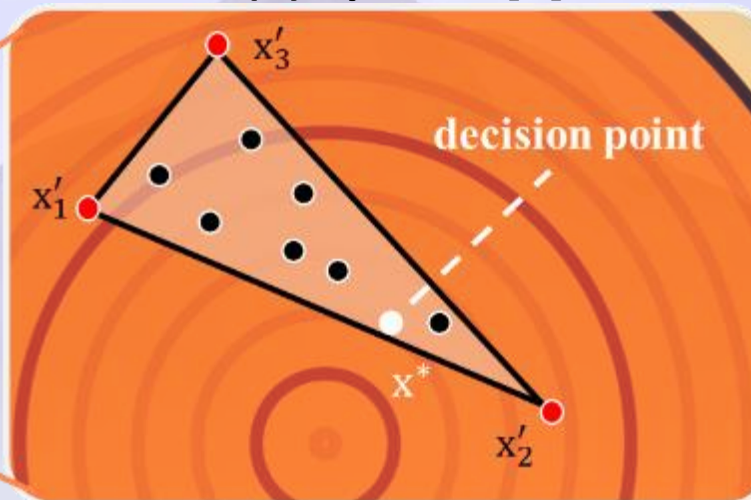
(b) opt-SDF [2]

Local minimum &  
Inefficient iteration

- ✓ High resolution
- ✓ Parallel-friendly
- ✓ Close to global minimum



(c) multi-res-SDF (ours)



[1] Distance fields for rapid collision detection in physically based modeling. In Proceedings of GraphiCon (Vol. 2003, pp. 58-65).

[2] Local optimization for robust signed distance field collision. Proceedings of the ACM on Computer Graphics and Interactive Techniques, 3(1), 1-17.





# PhysHand

## Sec4.1 Constraints

We first present the complete experimental results regarding constraints, contact, and deformation.

## 4. Experiments

### Deformation

Experiment on physical  
constraints

Loosing flesh

Attached flesh

Smooth skin



(a) +  $C^{\text{edge}}$  and  $C^{\text{tet}}$



(b) +  $C^{\text{att}}$

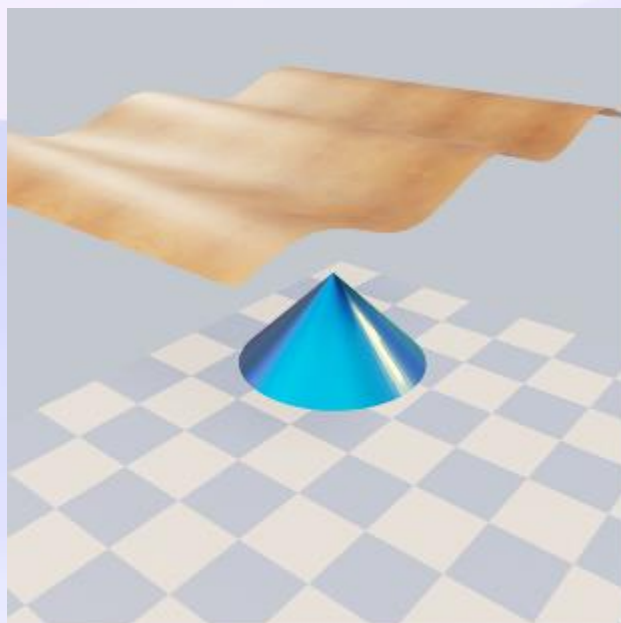


(c) +  $C^{\text{smo}}$

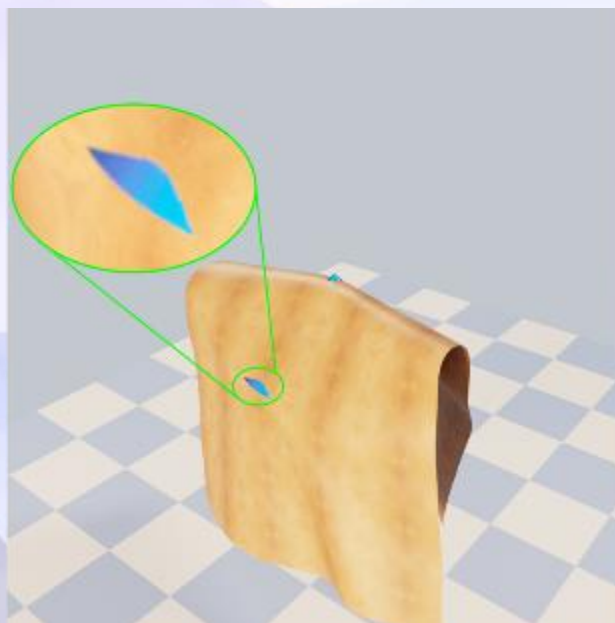
**Figure 6:** Improvements in deformation from layer-corresponding constraints. We gradually add constraints. (a) The hand with  $C^{\text{edge}}$  and  $C^{\text{tet}}$ . (b) The activation of  $C^{\text{att}}$ . (c) Enabling  $C^{\text{smo}}$ .

Contact

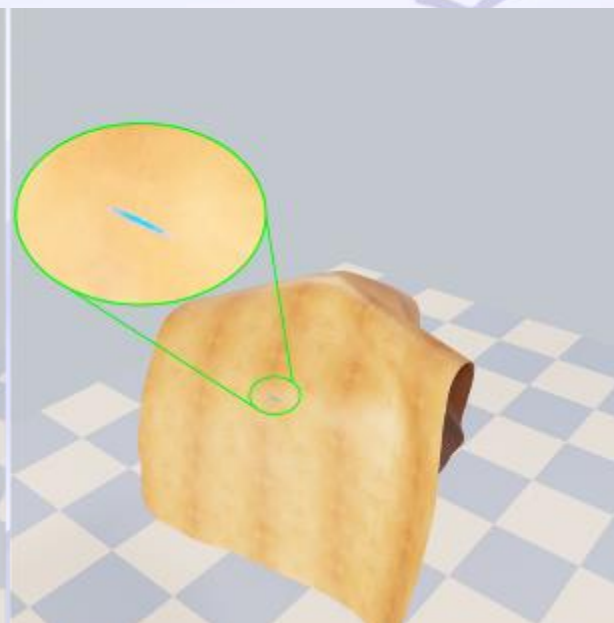
Qualitative comparison



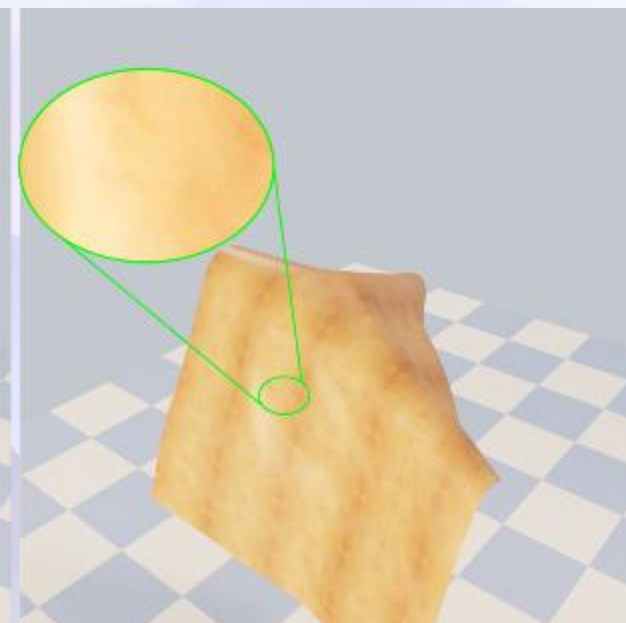
(a) Initialization



(b) vertex-SDF



(c) opt-SDF



(d) multi-res-SDF (ours)

We reproduce a typical simulation scenario carried out in [1], including a **cloth-like triangular mesh** and a **cone** represented as the **SDF**.

[1] Macklin, M., Erleben, K., Müller, M., Chentanez, N., Jeschke, S., & Corse, Z. (2020). Local optimization for robust signed distance field collision. Proceedings of the ACM on Computer Graphics and Interactive Techniques, 3(1), 1-17.

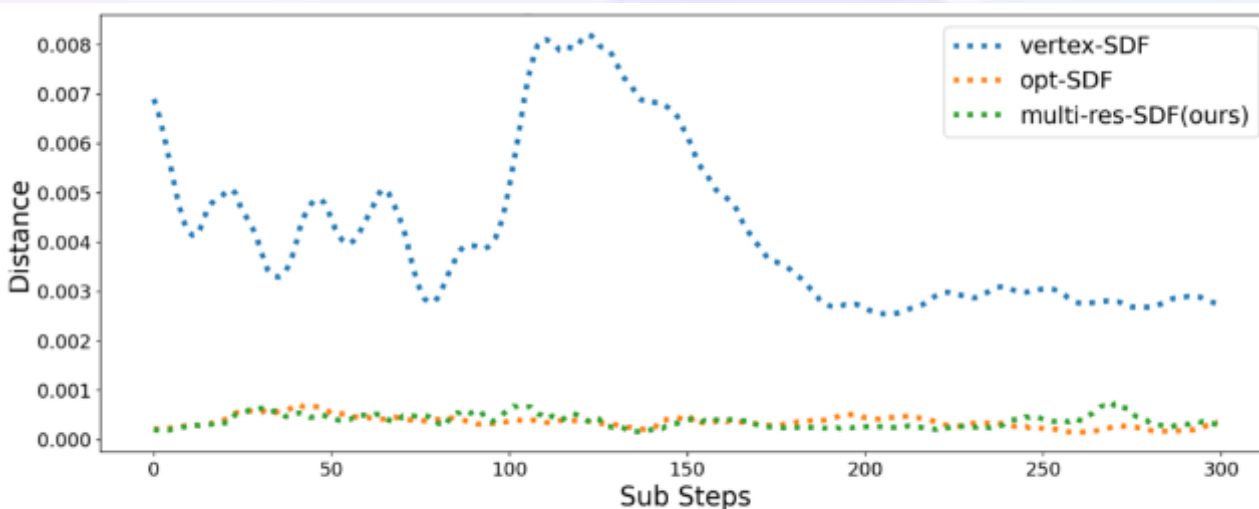


## 4. Experiments

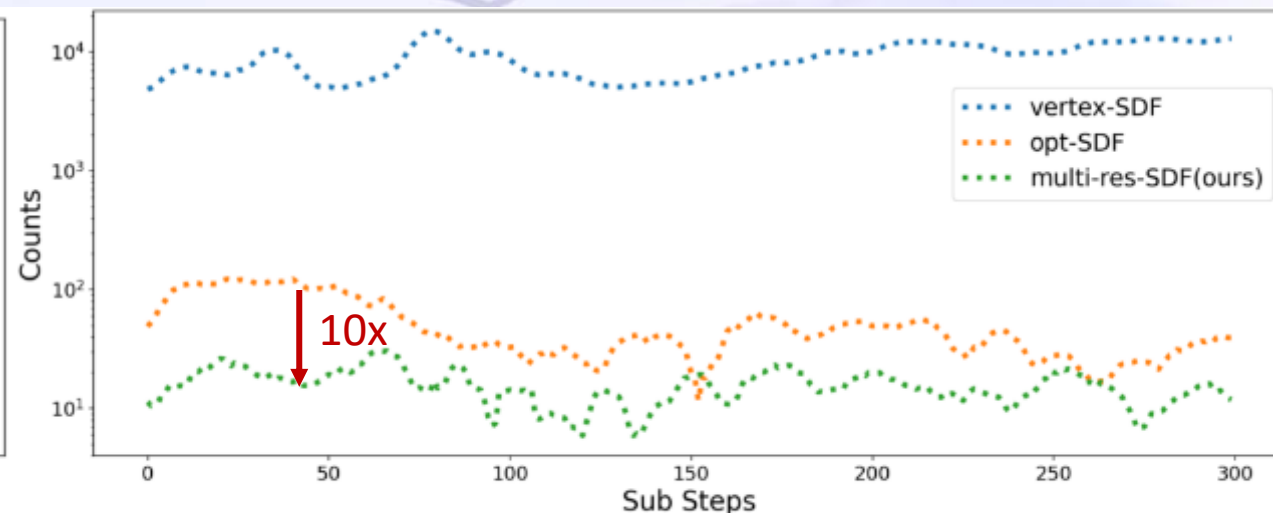


Contact

Quantitative comparison



(e) Average penetration distance



(f) Penetration count

(e) For Average penetration distance, **multi-res-SDF** performs comparably to **opt-SDF**.

(f) For Penetration count, **multi-res-SDF** achieves nearly **tenfold lower** penetration count than **opt-SDF**.

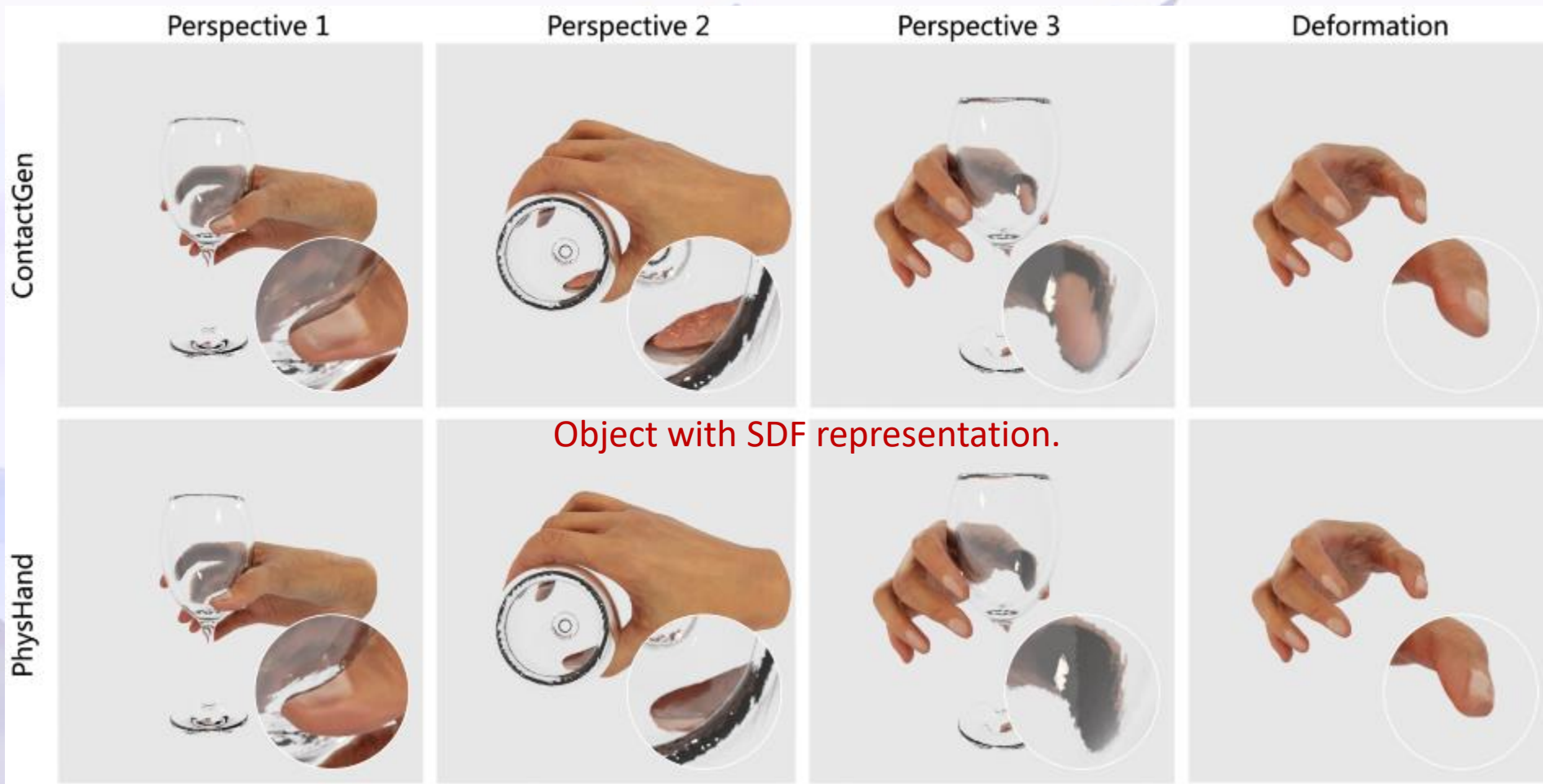
- It is exactly because **opt-SDF** has a higher number of penetrations that it reduces the average penetration distance.
- In **our approach**, since each iteration of querying is performed by **global sampling** on the corresponding triangle, our approach can approximate the **global optima**.



## 4. Experiments

### HOI

Experiments on HOI  
data generation

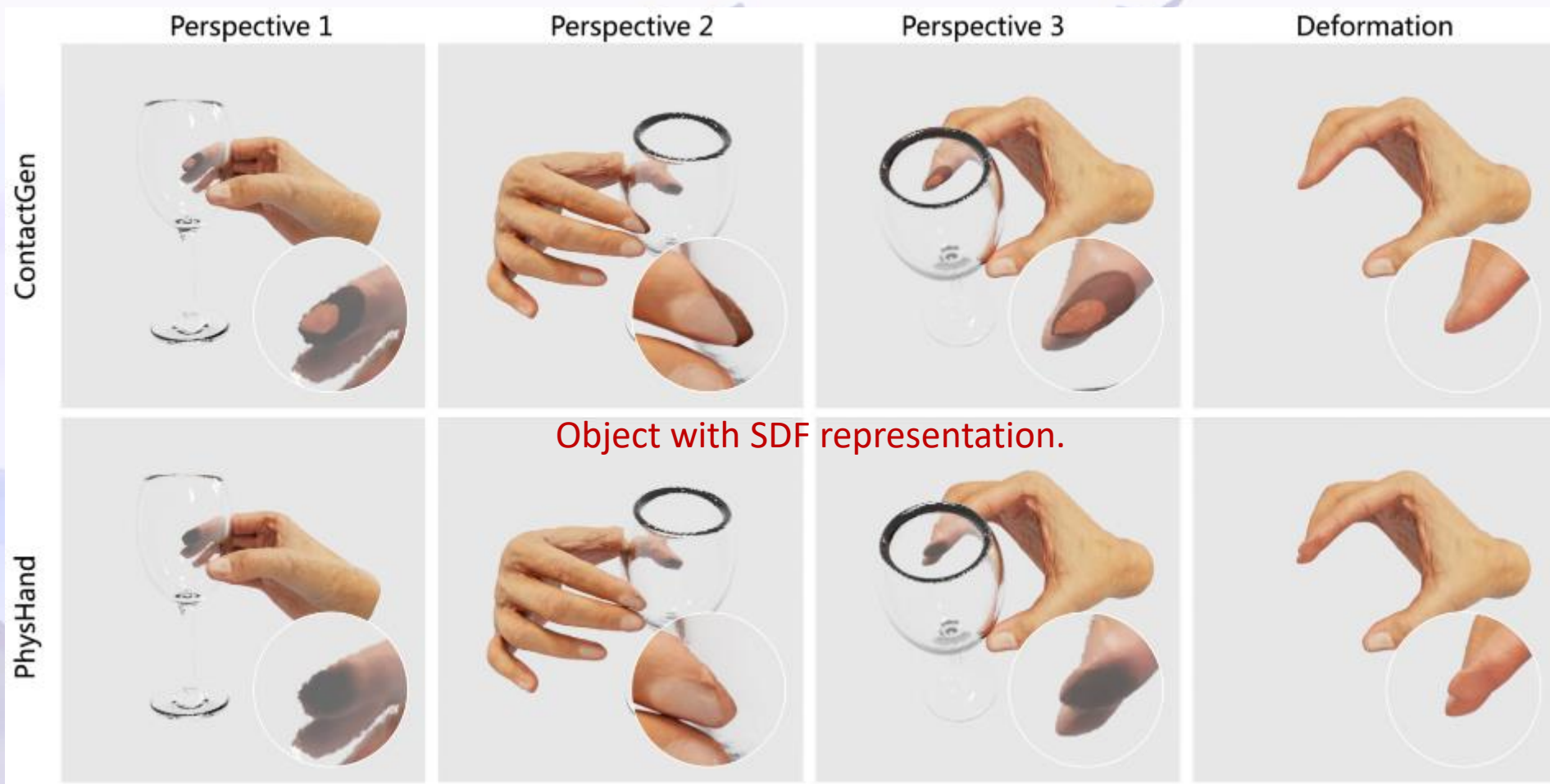


- We replicate ContactGen [1], a SOTA model in generating hand-object grasps.
- Despite ContactGen creating excellent grasps, there are obvious **penetrations**.
- PhysHand demonstrates its unique value by providing more authentic deformations and overcoming visible penetrations.

## 4. Experiments

### HOI

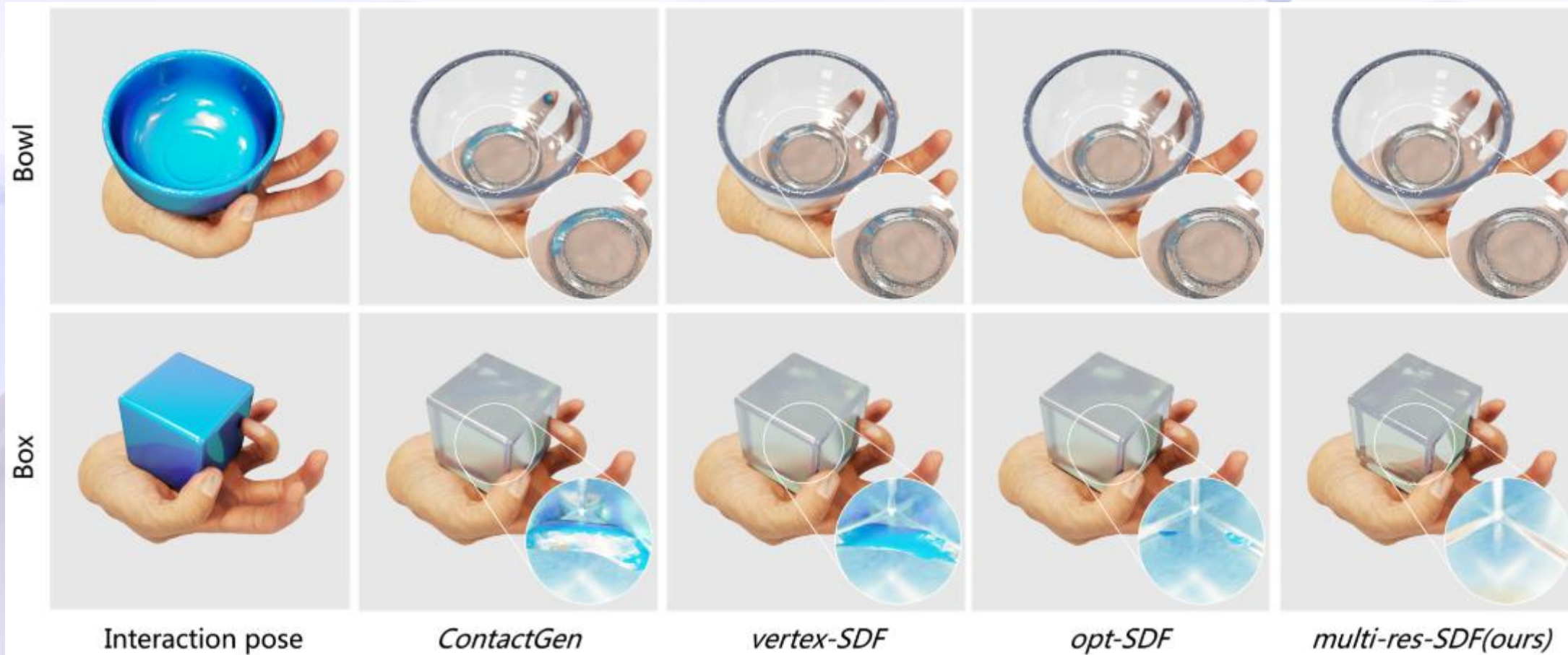
Experiments on HOI  
data generation



- We replicate ContactGen [1], a SOTA model in generating hand-object grasps.
- Despite ContactGen creating excellent grasps, there are obvious **penetrations**.
- PhysHand demonstrates its unique value by providing more authentic deformations and overcoming visible penetrations.

HOI

Quantitative comparison of different SDF-based contact handling strategy



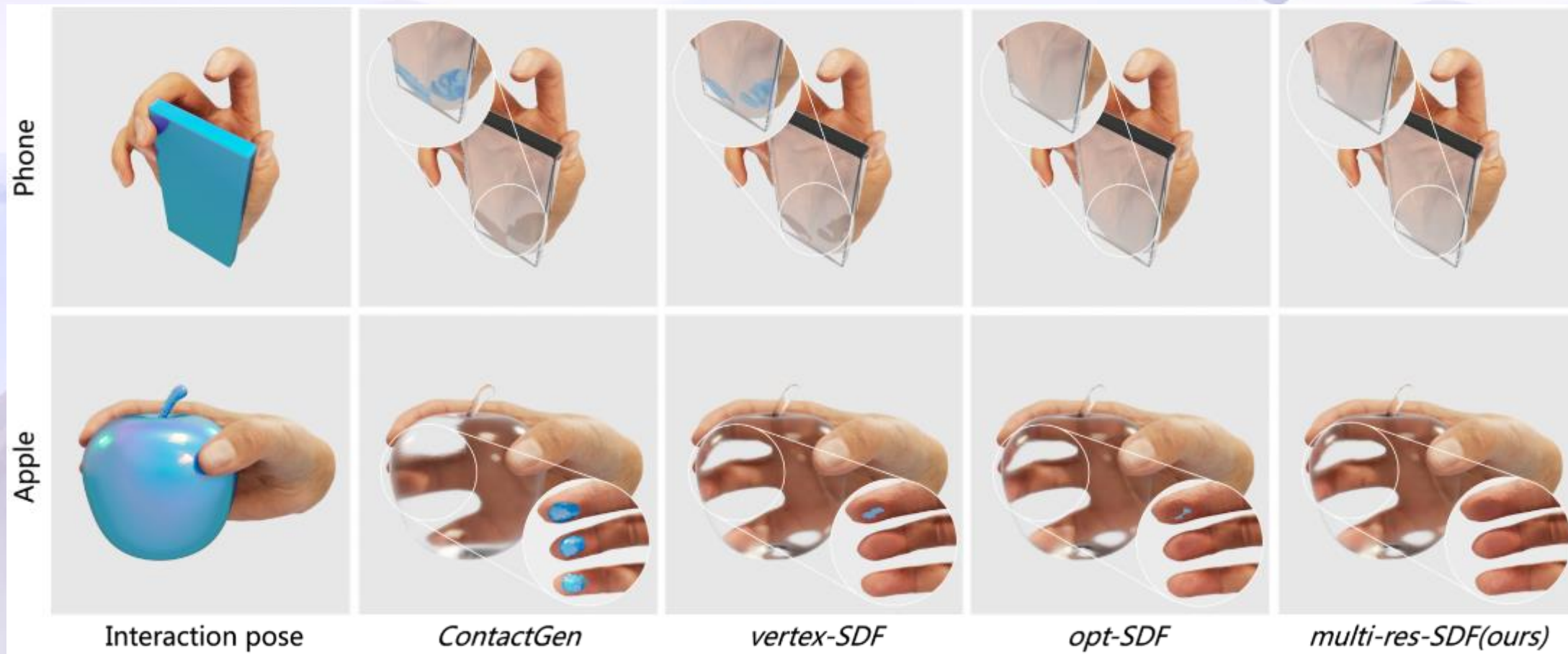
➤ The **dark blue regions** indicate **penetrations** in all graphs except for the first column.



## 4. Experiments

HOI

Quantitative comparison of different SDF-based contact handling strategy



➤ The **dark blue regions** indicate **penetrations** in all graphs except for the first column.



## 4. Experiments



### HOI

Quantitative comparison of contact methods in HOI experiments.

- Across all metrics of contacts, **our method** significantly surpasses other approaches with values approaching zero.
- **opt-SDF** does not support parallelization due to the **sequential** querying.
- Querying in **multi-res-SDF** is independent of each point, allowing for **parallel implementation**.

Object		ContactGen [LZY*23]	vertex-SDF [FSG03]	PhysHand opt-SDF [MEM*20]	multi-res-SDF (ours)
glass-1	count↓	143105	46285	156	<b>3</b>
	max ( $\mu\text{m}$ )↓	2503.9162	459.1479	6.2744	<b>0.2956</b>
	avg. ( $\mu\text{m}$ )↓	1305.9646	114.9909	1.9033	<b>0.2289</b>
	CPU/GPU time (ms)↓	-	<b>22/-</b>	246/-	2,517/27
glass-2	count↓	119067	63013	158	<b>1</b>
	max ( $\mu\text{m}$ )↓	2503.8602	442.6264	3.5655	<b>0.0500</b>
	avg. ( $\mu\text{m}$ )↓	1150.6618	206.9566	1.9978	<b>0.0500</b>
	CPU/GPU time (ms)↓	-	<b>21/-</b>	243/-	2,502/27
toothpaste	count↓	71033	27435	30	<b>1</b>
	max ( $\mu\text{m}$ )↓	3106.4365	2313.6602	7.4098	<b>0.0139</b>
	avg. ( $\mu\text{m}$ )↓	1068.7383	270.8561	1.7885	<b>0.0139</b>
	CPU/GPU time (ms) ↓	-	<b>21/-</b>	169/-	2,462/26
phone	count↓	287730	164933	2	<b>1</b>
	max ( $\mu\text{m}$ )↓	3323.5322	1916.7412	1.3571	<b>0.0103</b>
	avg. ( $\mu\text{m}$ )↓	1411.4840	70.8230	0.7542	<b>0.0103</b>
	CPU/GPU time (ms) ↓	-	<b>15/-</b>	227/-	1,095/12
apple	count↓	79827	37927	268	<b>0</b>
	max ( $\mu\text{m}$ )↓	3294.8354	189.9071	3.7722	<b>0</b>
	avg. ( $\mu\text{m}$ )↓	1219.7463	78.8565	1.0504	<b>0</b>
	CPU/GPU time (ms) ↓	-	<b>21/-</b>	220/-	1,995/24
bowl	count↓	86841	32120	190	<b>11</b>
	max ( $\mu\text{m}$ )↓	5718.0323	3129.6544	260.9675	<b>0.0427</b>
	avg. ( $\mu\text{m}$ )↓	1788.3155	845.0303	35.4007	<b>0.0093</b>
	CPU/GPU time (ms) ↓	-	<b>18/-</b>	145/-	1,480/16
box	count↓	163436	58827	820	<b>7</b>
	max ( $\mu\text{m}$ )↓	5217.0626	989.9247	0.4664	<b>0.0050</b>
	avg. ( $\mu\text{m}$ )↓	2331.5708	133.4961	0.0110	<b>0.0016</b>
	CPU/GPU time (ms) ↓	-	<b>17/-</b>	201/-	1,073/12



PG 2024  
Huangshan, China

## 4. Experiments

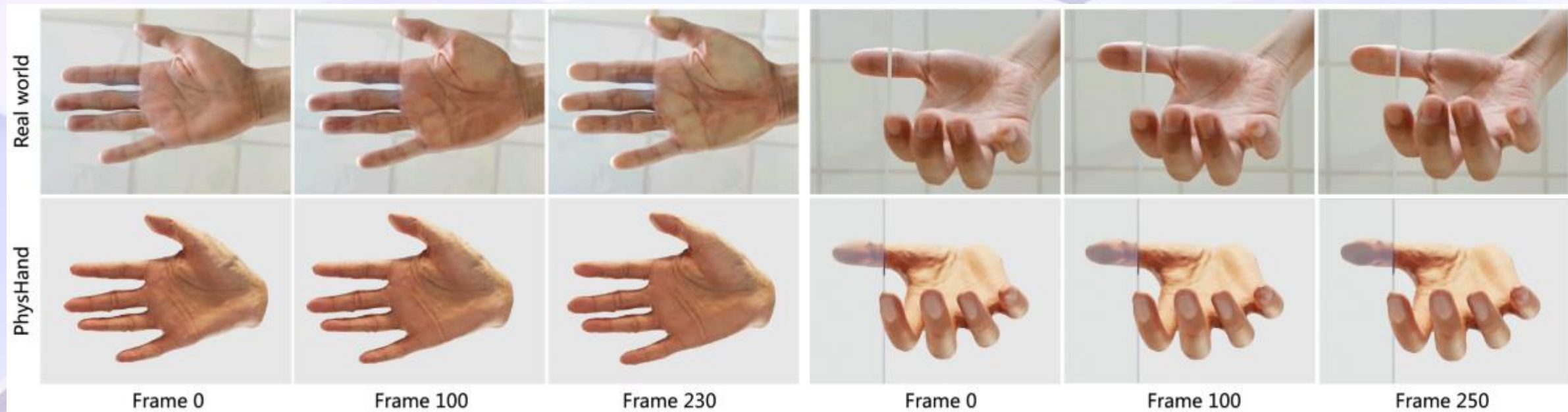


復旦大學  
FUDAN UNIVERSITY

TENCENT  
ROBOTICS X

HOI

Real world comparison



PhysHand is able to achieve deformations remarkably close to those observed in the real world.

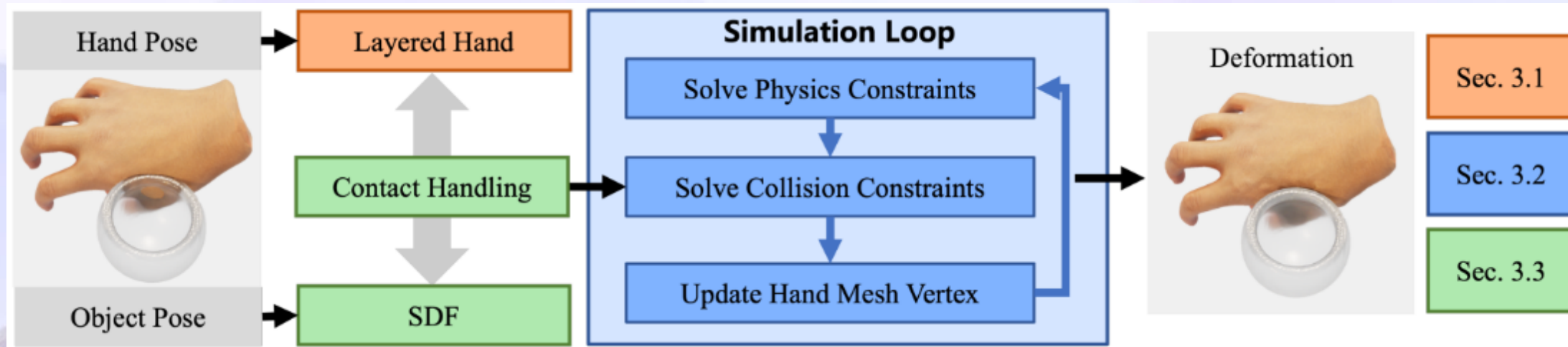




We present a novel hand simulation model, *PhysHand*, capable of faithfully reproducing the deformations in HOI.

### Contributions:

- A layered hand **geometry** containing the skin, flesh, and skeleton.
- Layer-corresponding **physics** formulas within a constraint-based dynamics framework.
- A multi-resolution querying strategy for accurate SDF-based **contact handling**.



### Limitations:

1. Since self-collision is not considered in this work, **self-penetration** between triangles might occur after solving the collision constraint.
2. PhysHand primarily focuses on deformation rather than actuation, thus we treat **muscles** and fat as the same soft tissue.
3. The absence of **friction** prevents PhysHand from actively grasping objects.

# *Thanks for attention!*

## PhysHand: A Hand Simulation Model with Physiological Geometry, Physical Deformation, and Accurate Contact Handling

Mingyang Sun<sup>†,1</sup> , Dongliang Kou<sup>†,1</sup> , Ruisheng Yuan<sup>1</sup> , Dingkang Yang<sup>1</sup> , Peng Zhai<sup>1</sup> , Xiao Zhao<sup>1</sup> ,  
Yang Jiang<sup>1</sup> , Xiong Li<sup>4</sup> , Jingchen Li<sup>†,4</sup> , and Lihua Zhang<sup>†,1,2,3</sup> 

<sup>1</sup>Academy for Engineering and Technology, Fudan University, Shanghai, China.

<sup>2</sup>Engineering Research Center of AI and Robotics, Ministry of Education, Changchun, China.

<sup>3</sup>Jilin Provincial Key Laboratory of Intelligence Science and Engineering, Changchun, China.

<sup>4</sup>Tencent Robotics X Lab, Shenzhen, China.

**Speaker:** Mingyang Sun (孙铭阳) [mysun21@fudan.edu.cn](mailto:mysun21@fudan.edu.cn)

**Colleague:** Dongliang Kou (寇栋梁) [dlkou23@m.fudan.edu.cn](mailto:dlkou23@m.fudan.edu.cn)

**Department:** Fudan University (复旦大学), Shanghai, China